Acoustic characteristics of the flow over different shapes of nozzle chevrons

Daniel CRUNTEANU*,[1,a], Petre-Claudiu COJAN[1,b]

*Corresponding author
*,[1] "POLITEHNICA" University of Bucharest, Faculty of Aerospace Engineering
Gh. Polizu Street 1-5, Bucharest, Romania
crunti_dani2005@yahoo.com

DOI: 10.13111/2066-8201.2013.5.3.6

Abstract: *The objective of this paper is to present a comparison between different types of chevrons and their influence on the acoustic power level radiated by the flow over them. The comparison was performed using a two-dimensional simulation of the flow over four different shapes of chevrons resulting propagation of the acoustic waves for each shape. Acoustic characteristics were revealed studying the main flow parameters (pressure, velocity, kinetic energy) in order to be able to discover the most efficient shape of chevron regarding the acoustic power level emitted.*

Key Words: *chevron, acoustic, noise, CFD, turbulence model, domain, mesh, boundary condition.*

1. INTRODUCTION

Numerical analysis of 2D steady air-flow over different types of nozzle chevrons was carried out using the commercial CFD (Computational Fluid Dynamics) software Ansys Fluent 12.1. For being able to run the simulation this software needs a pre-defined grid which was build using a pre-processor named Gambit 2.4.6. The evaluation of flow results were made using velocity and pressure field, turbulent characteristics and also acoustic characteristics (acoustic power level). The simulation of the sound waves propagation strongly depends on the accuracy of the numerical method used. Practically, high order accuracy methods are required for discretization. Because of this matter, for our Ansys Fluent simulations we have used the second-order upwind method, which is a more accurate one. After the results have been compared we have been able to reveal which is the most efficient shape of chevron regarding noise reduction.

2. PROBLEM FORMULATION

In order to prove the way in which the chevron shape influences the flow around it we proposed for study four different types of chevrons located in an unheated air stream at a velocity of 250 m/s. Table 1 describes the types of chevrons which have been taken into consideration.

For a real approach we have considered each chevron located inside of a closed domain which has been meshed using Gambit 2.4.6. An example of the domain dimensions is shown in Fig. 1.

[a] Lecturer PhD. eng.
[b] Eng.

Table 1 –Characteristics and dimension of the four chevrons (all dimensions are in centimeters)

Code	***Type of chevron***
CH-1	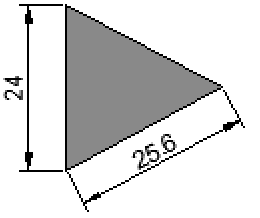
CH-2	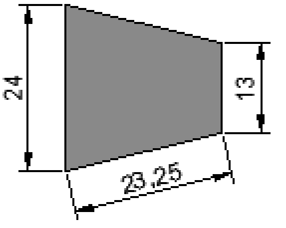
CH-3	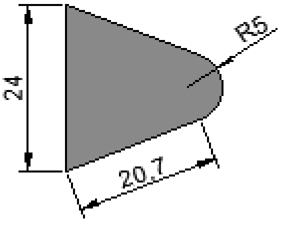
CH-4	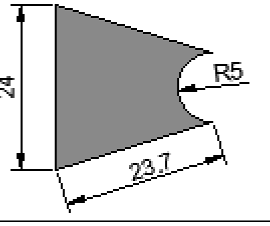

For the two-dimensional simulation of the flow, the governing equations for Ansys Fluent 12.1 are based on Navier-Stokes equations. The equations which describe the best our case are the following ones.

$$\frac{\partial \hat{\mathbf{U}}}{\partial t}+\frac{\partial \hat{\mathbf{F}}_{\xi}}{\partial \xi}+\frac{\partial \hat{\mathbf{F}}_{\eta}}{\partial \eta}=\frac{\partial \hat{\mathbf{G}}_{\xi}}{\partial \xi}+\frac{\partial \hat{\mathbf{G}}_{\eta}}{\partial \eta} \tag{7.1}$$

where $\hat{\mathbf{U}}=\frac{\mathbf{U}}{J}$, end

$$\hat{\mathbf{F}}_{\xi}=\frac{\xi_t\mathbf{U}+\xi_x\mathbf{F}_x+\xi_y\mathbf{F}_y}{J} \qquad \hat{\mathbf{F}}_{\eta}=\frac{\eta_t\mathbf{U}+\eta_x\mathbf{F}_x+\eta_y\mathbf{F}_y}{J}$$
$$\hat{\mathbf{G}}_{\xi}=\frac{\xi_x\mathbf{G}_x+\xi_y\mathbf{G}_y}{J} \qquad \hat{\mathbf{G}}_{\eta}=\frac{\eta_x\mathbf{G}_x+\eta_y\mathbf{G}_y}{J} \tag{7.2}$$

The viscous tensors are:

$$\tau_{xx} = \frac{2}{3}\frac{\mu}{\mathrm{Re}_\infty}\left[2\left(u_\xi \xi_x + u_\eta \eta_x\right) - \left(v_\xi \xi_y + v_\eta \eta_y\right)\right]$$

$$\tau_{yy} = \frac{2}{3}\frac{\mu}{\mathrm{Re}_\infty}\left[2\left(v_\xi \xi_y + v_\eta \eta_y\right) - \left(u_\xi \xi_x + u_\eta \eta_x\right)\right] \quad (7.3)$$

$$\tau_{xy} = \frac{\mu}{\mathrm{Re}_\infty}\left(u_\xi \xi_y + u_\eta \eta_y + v_\xi \xi_x + v_\eta \eta_x\right)$$

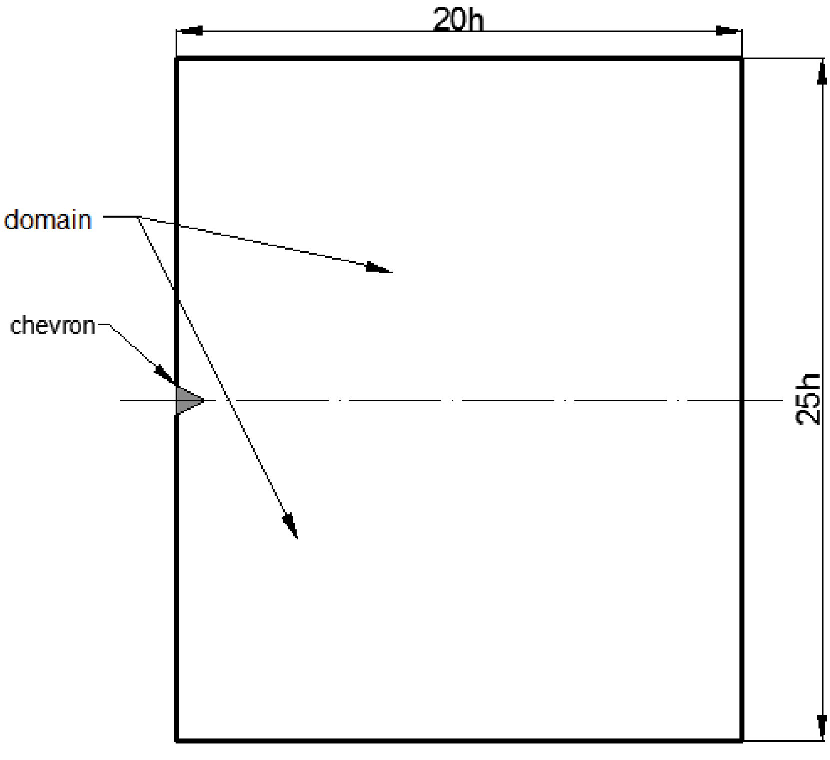

Fig. 1 – Studying domain (h-chevron's length)

3. NUMERICAL SIMULATION AND RESULTS

On the first hand we placed each chevron inside the studying domain and after that we realized a mesh for each case using Gambit 2.4.6.

The resulted meshes were structured ones. They were made selecting *Map* option for the type of mesh and *Quad* option for the elements. They also contain around 2.5×10^5 faces and 12000 nodes.

For obtaining proper results we chose to make a denser grid next to the chevron's walls. This option is justified because our interest is confined to find best results close to the chevron area.

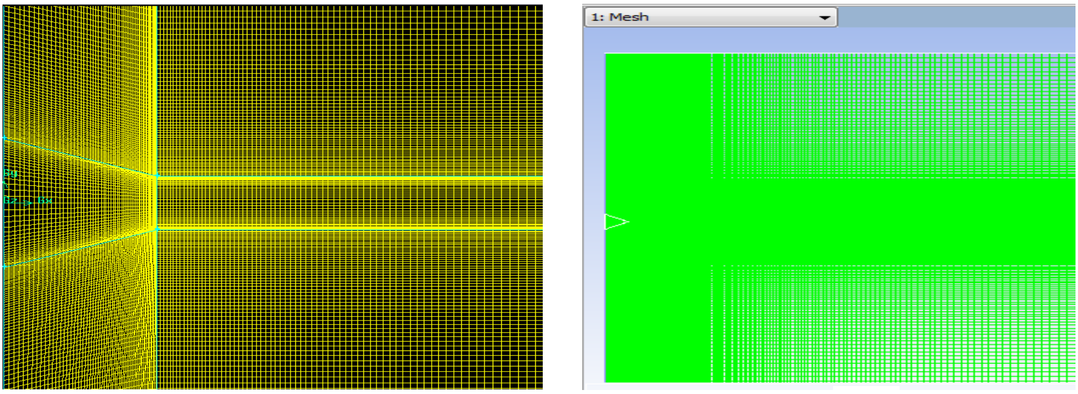

a) b)

Fig. 2 – Structured meshes: a) Gambit 2.4.6; b) Ansys Fluent 12.1

Because we were looking for a higher accuracy of the solution we have selected a double-precision method and *density-based* solver because this was originally designed for high-speed flows.

The density-based explicit and implicit formulations solve the equations for additional scalars (e.g. turbulence or radiation quantities) sequentially.

The implicit and explicit density-based formulations differ in the way that they linearize the coupled equations.

Due to broader stability characteristics of the implicit formulation, a converged steady-state solution can be obtained much faster using the implicit formulation rather than the explicit formulation.

However, the implicit formulation requires more memory than the explicit formulation. The governing equation for density-based solver which involves a scalar quantity ϕ is the following one:

$$\int_V \frac{\partial \rho\phi}{\partial t} dV + \oint \rho\phi \mathbf{v} \cdot d\mathbf{A} = \oint \Gamma_\phi \nabla \phi \cdot d\mathbf{A} + \int_V S_\phi dV \qquad (7.8)$$

where: ρ -density;

$\mathbf{v}$ -velocity vector ($\mathbf{v} = u\mathbf{i} + v\mathbf{j}$, for 2D);

$\mathbf{A}$ -area vector;

Γ_ϕ -diffusion coefficient for ϕ;

$\nabla\phi$ -gradient of ϕ ($\nabla\phi = \frac{\partial\phi}{\partial x}\mathbf{i} + \frac{\partial\phi}{\partial y}\mathbf{j}$, for 2D);

S_ϕ -source of ϕ.

Regarding boundary conditions we selected the following types for all of our four simulations:

- WALL (solid walls) –for the chevron profile;
- VELOCITY-INLET (250 m/s) –for the inlet area;
- PRESSURE-OUTLET –for lateral and outlet area.

Because we searched for accuracy results regarding the acoustic field, we enabled the *Broadband Acoustic Source.*

This model uses for calculation Proudman's equation, Lilley's equation and Goldstein's theory. All these approaches are based on Lighthill's equation for turbulent flows, which tells us that the acoustic power emitted by a spherical source is:

$$P(y)=\frac{K\rho_0 u'^4 l^3}{4\pi a_0^5 \tau_\xi^4}\frac{1+M_c^2}{\left(1-M_c^2\right)^4} \tag{4.21}$$

Beside this we needed to select a proper turbulence model which should be a characteristic of each flow.

Our option was standard k-epsilon turbulence model because this is one of the most popular models which have been tested for a large area of applications. One of his major advantages is the fact that this model doesn't need a large amount of time for doing the simulation.

This is the reason why our simulations had a convergent solution somewhere between 28000 and 30000 iterations, the maximum time spent for a complete simulation being around 36 hours.

The obtained results, shown in the next figures, took into consideration the fact that noise production is closely connected with flow velocity and turbulent kinetic energy.

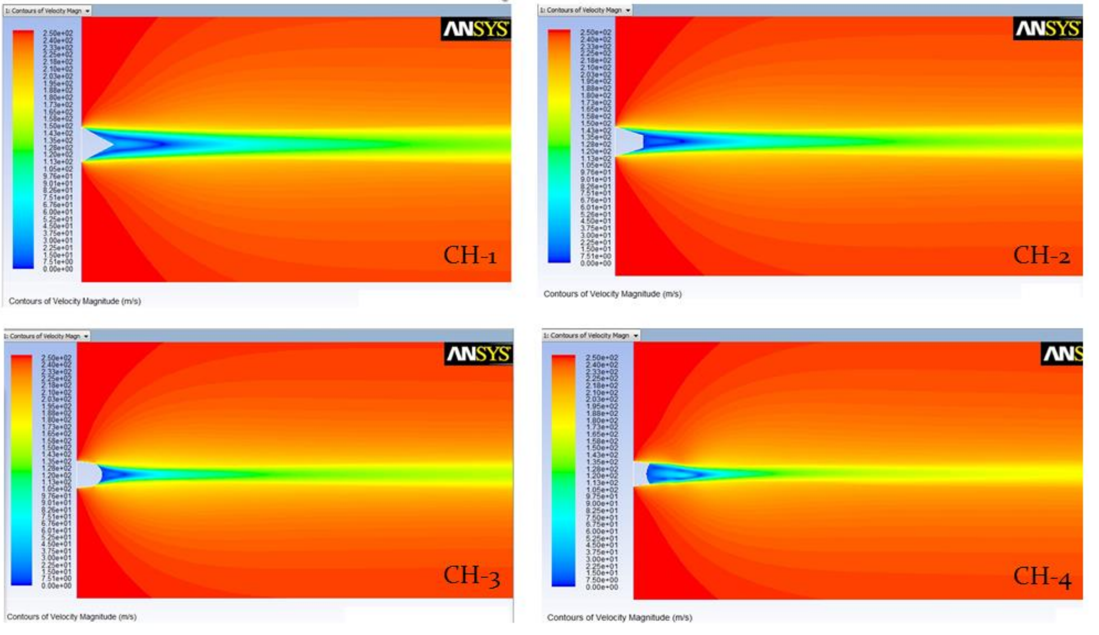

Fig. 3 – Contours of Velocity Magnitude (m/s)

As we can see in Fig. 3, the chevron shape does not have quite an influence regarding air flow velocity.

So, taking into consideration that the noise magnitude is proportional with the air flow velocity, for now we cannot tell which of the shapes is more efficient in noise reduction.

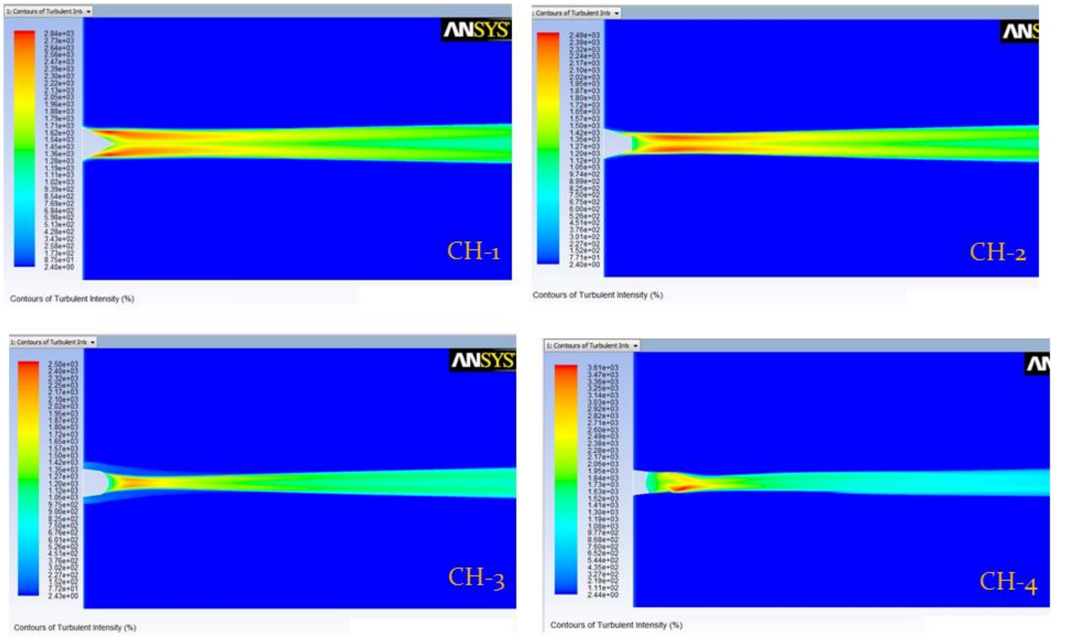

Fig. 4 – Contours of Turbulent Intensity (%)

Studying the turbulent intensity we can observe that the chevron shapes with the lower intensity are CH-2 and CH-3. So these two shapes should be taken into consideration for the following studies which involve noise reduction.

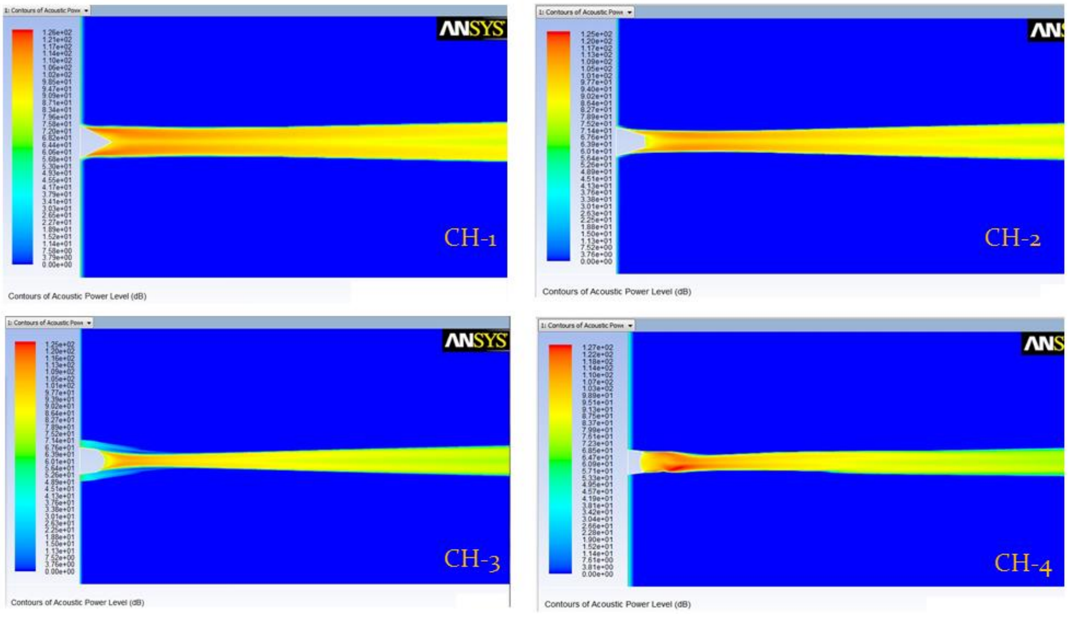

Fig. 5 – Contours of Acoustic Power Level (dB)

Going further and analyzing the acoustic power level we can find a difference of two decibels between chevrons CH-2, CH-3 (125 dB) and chevron CH-4 (127 dB), and a difference of one decibel between chevrons CH-2, CH-3 (125 dB) and chevron CH-1 (126 dB).

4. CONCLUSIONS

In this numerical simulation the importance of the air flow velocity and turbulence effects on the acoustic noise generation and propagation was obviously presented. Beside this, we also presented the influence of chevron shape design on the acoustic noise reduction, finding that this aspect may contribute to a decrease of acoustic power level by 2 dB.

The technology which has been used for simulation was not a very high one, this being the reason why the differences between the four shapes of chevrons are not so evident. Despite this, we can tell that the most efficient shape of chevron, from all points of view (noise reduction, turbulent intensity and air flow velocity) is chevron CH-3.

REFERENCES

[1] E. Marvin Goldstein, *Aeroacustics,* McGraw-Hill International Book Company, New York, USA, 1976.

[2] S. Sarkar, M. Y. Hussaini, Computation of the sound generated by isotropic turbulence, *NASA Contractor Report 191543, ICASE Report No. 93-74*, October 1993.

[3] Umesh Paliath, *Numerical simulation of jet noise,* ISBN 0542810077, 9780542810077, Pennsylvania State University, USA, 2006.

[4] F. Alton Everest, *The master handbook of acoustics, fourth edition,* McGraw-Hill International Company, SUA, 2001.

[5] C. K. W. TAM, *Numerical Methods in Computational Aeroacoustics,* AIAA Short Course, Seattle, Washington 8-9 May 1999.

[6] T. J. CHUNG, *Computational fluid dynamics,* ISBN 0521594162, Cambridge University Press, New York, 2002.

[7] ***, ANSYS FLUENT 12.1 documentation.

[8] Vance Dippold III, *CFD Analyses and Jet-Noise Predictions of Chevron Nozzles with Vortex Stabilization,* Glenn Research Center, Cleveland, Ohio, USA, 2008.